

# A method for smoothing Impulse Response Functions for discrete-time linear models

Gray Calhoun\*

2016-03-29, v0.3-2-gd692bcd

## Abstract

We show how to construct continuous and differentiable Impulse Response Functions for discrete-time Vector Autoregressions and Vector Error-Correction Models. Current methods produce piecewise linear functions that introduce visual distortions, especially when many response functions are plotted in the same graph to represent uncertainty or partial identification. We also show how to plot the cumulative response to a shock and incorporate moving average dynamics.

## Contents

1	Introduction . . . . .	2
2	Method for smoothing IRFs . . . . .	2
2.1	AR(1) motivation . . . . .	3
2.2	General Approach for VAR( $p$ ) . . . . .	6
2.3	Finite-order linear models . . . . .	9
3	Examples . . . . .	11
3.1	Numerical example . . . . .	12
3.2	Empirical analysis of the effect of monetary policy . . . . .	13
4	Conclusion . . . . .	15
	References . . . . .	19
A	Appendix: Changes to this paper from previous versions . . . . .	20

---

\*Economics Department, Iowa State University; gcalhoun@iastate.edu, web: <http://gray.clhn.org>. Helle Bunzel, Seth Pruitt, and participants in the ISU Statistical Graphics Working Group gave very helpful feedback on early versions of this paper.

## 1 Introduction

Impulse Response Functions (IRFs) are widely used in macroeconomics to represent the dynamic effect over time of an unanticipated shock. If  $y_t$  is a stationary sequence of random vectors, an IRF is a graph of the change in the conditional expectation of  $y_{t+s}$  in response to an unanticipated shock to  $y_t$ , plotted as a function of  $s$ . The conditional expectation may be implied by a theoretical model or a statistical model, such as a VAR, in which case additional assumptions may be necessary to identify the shocks of economic interest. In either of these cases, IRFs can provide a parsimonious and interpretable summary of the key features of the model.

Producing an IRF requires calculating the conditional expectation  $E_t y_{t+s}$  under different counterfactual scenarios, with and without the shock of interest. Since most macroeconomic models are defined and estimated in discrete time (both  $t$  and  $s$  are integers) the conditional expectations used to produce IRFs are calculated in discrete time as well. (See Chapter 1 of Hamilton, 1994, for example.) But in most applications, it is desirable to graph the IRFs as curves and connect the points between the integer values of  $s$ ; this is especially important when more than one IRF is plotted on the same graph — whether to represent dynamics under different assumptions (see Bernanke and Mihov, 1998, and Stock and Watson, 2001, for representative examples), to represent statistical uncertainty (Kilian, 1998, and Sims and Zha, 1999) or to represent regions that are partially identified (Uhlig, 2005, and Inoue and Kilian, 2013). Currently, this is done by linear interpolation between the integer values of  $E_t y_{t+s}$  but this practice has some drawbacks. Linear interpolation introduces misleading visual distortions and can remove potentially interesting dynamics from the model.

In this paper, we show how to construct continuous and smooth IRFs for vector ARMA and other linear time series models. These IRFs are defined for all values of  $t$  and  $s$ , even noninteger values, and ensure that the interpolation obeys the same dynamics as the rest of the model. The resulting graph removes the distortions introduced by current methods. Section 2 presents these results, Section 3 provides some numeric and empirical examples, and Section 4 concludes.

## 2 Method for smoothing IRFs

This section presents the main results of the paper: smooth IRFs for finite-order linear models. Section 2.1 presents results for the AR(1) to motivate our approach. Section 2.2 extends this result to finite-order VARs and Section 2.3 extends the result further to

VARMA and VECM models and to cumulative responses. The rest of this subsection introduces some notation and defines the IRFs formally.

Let  $\{\gamma_t\}$  be a stationary sequence of random vectors in  $\mathbb{R}^k$ , let  $\mathcal{F}_t$  represent the information set available in period  $t$ ,

$$\mathcal{F}_t = \sigma(\gamma_t, \gamma_{t-1}, \gamma_{t-2}, \dots),$$

and let the function  $m_s$  represent the conditional expectation of  $\gamma_{t+s}$  given  $\gamma_t$ , so

$$m_s(x) = E(\gamma_{t+s} \mid \gamma_t = x)$$

for each  $s \geq 0$ . Define  $m_s = 0$  for  $s < 0$  and let  $E \gamma_t = \mu$ . For a shock of interest  $u$ , with  $u \in \mathbb{R}^k$ , the IRF corresponding to  $u$  is the function

$$\Psi_u(s) = E(m_s(\gamma_t + u) - m_s(\gamma_t)). \quad (1)$$

The shock,  $u$ , in these equations should be viewed as the “reduced form” version of the shock — an unanticipated change in the current value of  $\gamma_t$ . In a Structural VAR application,  $u$  will typically be related to a more fundamental shock of economic interest  $\delta$  through the linear transformation  $u = \Gamma\delta$ , for some known or estimated matrix  $\Gamma$ .

If  $\gamma_t$  is nonstationary  $E_t$  may depend on the value of  $t$ . In that case, define

$$m_{ts}(x_0, \dots, x_p) = E(\gamma_{t+s} \mid \gamma_t = x_0, \dots, \gamma_{t-p} = x_p)$$

and let

$$\Psi_{tu}(s) = m_{ts}(E \gamma_t + u, E \gamma_{t-1}, \dots, E \gamma_{t-p}) - m_{ts}(E \gamma_t, E \gamma_{t-1}, \dots, E \gamma_{t-p}).$$

Note that  $\Psi_{tu}$  can be independent of  $t$  even if  $m_{ts}$  is not.

## 2.1 AR(1) motivation

For motivation, start with the simplest univariate case and assume that  $\gamma_t$  is the AR(1)

$$\gamma_t = a\gamma_{t-1} + \varepsilon_t \quad (2)$$

where  $\varepsilon_t$  is a martingale difference sequence and  $|a| < 1$ . For discrete-time models, it is easy to define the IRF recursively and  $\Psi_h(s) = a^s u$ . When  $a > 0$ , this function is well-defined for all positive real  $s$ , and can be used directly to interpolate between the

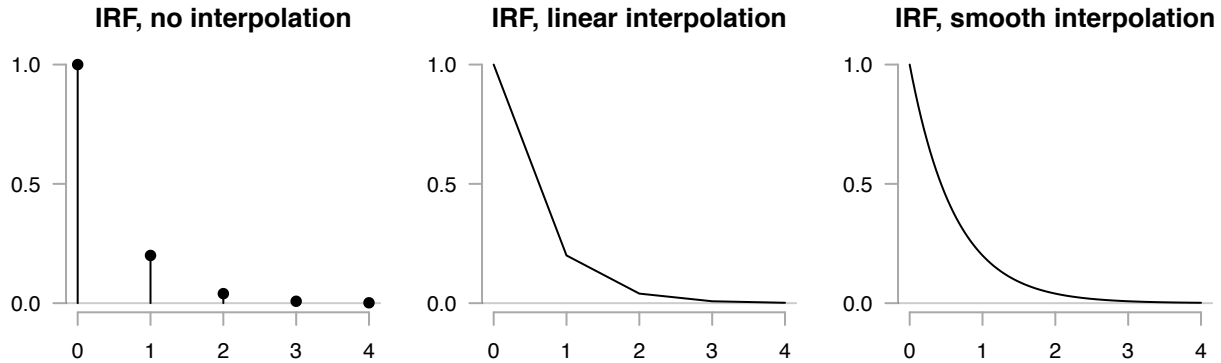


Figure 1: IRF for simple AR(1) example. Here  $\gamma_t = 0.2\gamma_{t-1} + \varepsilon_t$  — the vertical axis shows  $\Psi_1(s)$ . The left panel plots only integer values of  $s$ , the middle panel uses linear interpolation between the integers, and the right panel plots the function  $0.2^s$  directly.

integer points. But typically representing these dynamics has been achieved by linear interpolation, so

$$\Psi_u(s) = (s - \lfloor s \rfloor)\Psi_u(\lfloor s \rfloor + 1) + (1 - s + \lfloor s \rfloor)\Psi_u(\lfloor s \rfloor) \quad (3)$$

$$= (s - \lfloor s \rfloor)a^{\lfloor s \rfloor+1}u + (1 - s + \lfloor s \rfloor)a^{\lfloor s \rfloor}u \quad (4)$$

for noninteger  $s$ , where  $\lfloor s \rfloor$  is the largest integer less than or equal to  $s$ .

Figure 1 plots  $\Psi_u(s)$  for  $u = 1$  and  $a = 0.2$  using three approaches: first only for the integer values of  $s$ , second using linear interpolation between the integer values defined by (4), and finally using  $a^s u$  directly for all  $s \geq 0$ .<sup>1</sup> While one could debate which of the functions represents the ‘true’ impact of a shock at a fractional point in time and whether the interpolated points should be interpreted, the dynamics and rate of decay of the AR model are much more clearly represented by the right panel that graphs  $0.2^s$  directly.

This should not be surprising. We can see that  $\Psi_u(s) = a^s u$  satisfies the recurrence relation implied by the lag structure of the original AR process for any positive real value of  $s$ :

$$\Psi_u(s) = a^s u = a \times a^{s-1} u = a \Psi_u(s-1). \quad (5)$$

Letting  $\Phi(L)$  define the lag polynomial of the AR(1) defined by Equation (2), (so the autoregressive model is defined as  $\Phi(L)\gamma_t = \varepsilon_t$  for all  $t$ ) we can express (5) in a form

---

<sup>1</sup>All of the graphs in this paper were produced using R. (R Development Core Team, 2011)

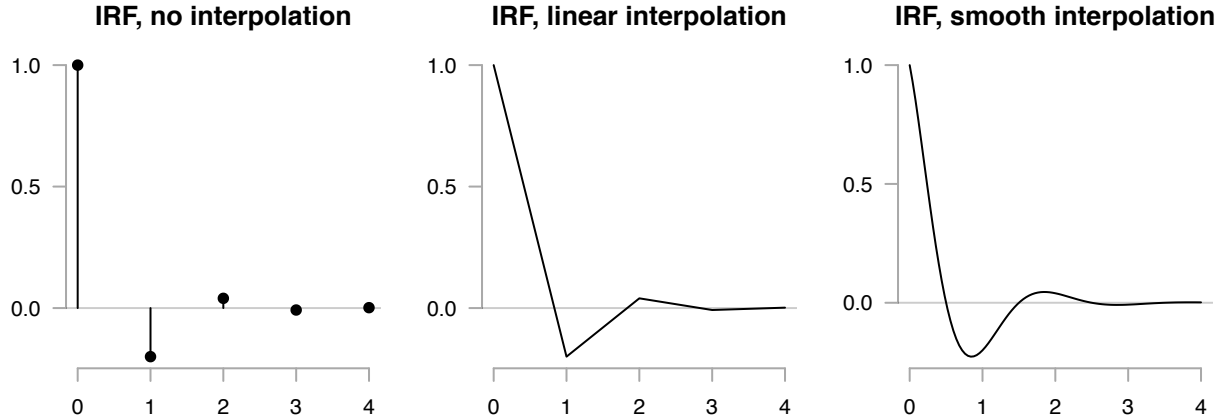


Figure 2: IRF for simple AR(1) example. Here  $y_t = -0.2y_{t-1} + \varepsilon_t$  — the vertical axis shows  $\Psi_s(1)$ . The left panel plots only integer values of  $s$ , the middle panel uses linear interpolation between the integers, and the right panel plots the function  $|a|^s \cos(\pi s)$  directly.

that will be easier to extend to more complicated DGPs,

$$\Phi(L)\Psi_u(s) = (1 - aL)\Psi_u(s) = 0 \quad (6)$$

for all  $s \in \mathbb{R}^+$  with the implicit definition  $L\Psi_u(s) = \Psi_u(s - 1)$ . When  $\Psi_u(s)$  is constructed by linear interpolation, i.e. (4), the recursive relationships (5) and (6) only hold for integer values of  $s$ .

The case  $a \in (-1, 0)$  is slightly more complicated. The previous solution,  $a^s u$ , is well-defined and real-valued only for integer values of  $s$ , so it can no longer be used directly for interpolation between the noninteger points. Instead, consider the definition

$$\Psi_u(s) = |a|^s \cos(\pi s) \cdot u. \quad (7)$$

For integer values of  $s$ ,  $\cos(\pi s) = 1$  so (7) is exactly equal to  $a^s u$ . But (7) remains real-valued and well defined for noninteger  $s$  as well. Moreover, (7) satisfies the recurrence relation for the AR(1) model for all values of  $a \in (-1, 1)$

$$\Psi_u(s) = |a|^s \cos(\pi s) \cdot u = -|a| \times |a|^{s-1} \cos(\pi(s-1)) \cdot u = a \Psi_u(s-1)$$

implying that

$$\Phi(L)\Psi_u(s) = (1 - aL)\Psi_u(s) = 0$$

as before. Figure 2 plots the IRFs for  $a = -0.2$  and  $u = 1$  with no interpolation, linear

interpolation, and the definition (7). Just as before, the smooth version more accurately reflects the system's dynamics after a shock.

This choice of  $\Psi_u(s)$  was not made at random. Any complex number  $a + bi$  can be written in polar form,

$$a + bi = R[\cos(\theta) - i \sin(\theta)]$$

where  $R = |a^2 + b^2|^{1/2}$  and  $\theta$  satisfies  $\cos(\theta) = a/R$  and  $\sin(\theta) = b/R$ . Real powers of  $a + bi$  can be expressed as<sup>2</sup>

$$(a + bi)^s = R^s[\cos(\theta s) - i \sin(\theta s)].$$

For the AR example above,  $a < 0$  and  $b = 0$  so  $\theta = \pi$ . Then  $a^s = |a|^s \cos(\pi s)$  as we originally claimed.

This example also suggests a more general method for interpolating between integer values of  $s$  for any VAR; solve recurrence relation using standard tools (as described in Hamilton, 1994, for example) and use the solution as the IRF for real-valued  $s$ . We pursue that approach in the next section.

## 2.2 General Approach for VAR( $p$ )

The AR(1) model in the previous section can be extended to general VARs using the “canonical” representation.<sup>3</sup> Define  $y_t$  to be the VAR( $p$ ),

$$y_t = \sum_{j=1}^p A_j y_{t-j} + \varepsilon_t.$$

(We assume that  $y_t$  has mean zero to simplify the presentation without loss of generality.) To represent this relationship as a VAR(1), form the vector  $(y'_t, \dots, y'_{t-p+1})'$  and

---

<sup>2</sup>See Hamilton (1994) for background on complex numbers.

<sup>3</sup>See Hamilton (1994) or Hansen and Sargent (2013) for a textbook treatment of much of this material. Our presentation borrows heavily from Hamilton (1994).

observe that

$$\underbrace{\begin{pmatrix} y_t \\ y_{t-1} \\ y_{t-2} \\ \vdots \\ y_{t-p+1} \end{pmatrix}}_{Z_t} = \underbrace{\begin{pmatrix} A_1 & A_2 & \cdots & A_{p-1} & A_p \\ I_k & 0 & \cdots & 0 & 0 \\ 0 & I_k & \cdots & 0 & 0 \\ \vdots & \vdots & \ddots & \vdots & \vdots \\ 0 & 0 & \cdots & I_k & 0 \end{pmatrix}}_F \underbrace{\begin{pmatrix} y_{t-1} \\ y_{t-2} \\ \vdots \\ y_{t-p+1} \\ y_{t-p} \end{pmatrix}}_{Z_{t-1}} + \underbrace{\begin{pmatrix} \varepsilon_t \\ 0 \\ 0 \\ \vdots \\ 0 \end{pmatrix}}_{U_t}. \quad (8)$$

So this relationship is equivalent to  $Z_t = FZ_{t-1} + U_t$ . The conditional expectation has a convenient form that is trivial to calculate for integer values of  $s$ ,

$$m_s(x) = e_{1p}F^s x$$

where  $e_{jp}$  is the  $kp \times k$  selection matrix

$$e_{jp} = \begin{pmatrix} 0_{k \times (j-1)p} & I_k & 0_{k \times (k-j)p} \end{pmatrix}.$$

Consequently, for integer values of  $s$ , the IRF has the form

$$\Psi_u(s) = e_{1p}F^s e'_{1p} u.$$

This section will argue that a variation of this definition remains meaningful for noninteger values of  $s$ .

To show this, notice that, since  $F$  is square, it has the Jordan decomposition

$$F = M J M^{-1} \quad (9)$$

where  $J$  is block diagonal of the form

$$J = \begin{pmatrix} J_1 & \cdots & 0 \\ \vdots & \ddots & \vdots \\ 0 & \cdots & J_q \end{pmatrix}$$

and  $q$  is the number of unique eigenvalues of  $J_\ell$ . Each  $J_\ell$  is an  $n_\ell \times n_\ell$  matrix of the

form

$$J_\ell = \begin{pmatrix} \lambda_\ell & 1 & 0 & \cdots & 0 & 0 \\ 0 & \lambda_\ell & 1 & \cdots & 0 & 0 \\ 0 & 0 & \lambda_\ell & \cdots & 0 & 0 \\ \vdots & \vdots & \vdots & \ddots & \vdots & \vdots \\ 0 & 0 & 0 & \cdots & \lambda_\ell & 1 \\ 0 & 0 & 0 & \cdots & 0 & \lambda_\ell \end{pmatrix}$$

where  $\lambda_1, \dots, \lambda_q$  are the distinct eigenvalues of  $F$  and  $n_\ell$  is the number of times the  $\ell$ th eigenvalue is repeated. If all of the eigenvalues of  $F$  are distinct, (9) is just the eigenvalue decomposition of  $F$ .

This representation is convenient because, for positive integer values of  $s$ , we have

$$F^s = MJ^sM^{-1}$$

and

$$J^s = \begin{pmatrix} J_1^s & \cdots & 0 \\ \vdots & \ddots & \vdots \\ 0 & \cdots & J_q^s \end{pmatrix}, \quad J_\ell^s = \begin{pmatrix} h_\ell(s, 0) & h_\ell(s, 1) & h_\ell(s, 2) & \cdots & h_\ell(s, n_\ell) \\ 0 & h_\ell(s, 0) & h_\ell(s, 1) & \cdots & h_\ell(s, n_\ell - 1) \\ 0 & 0 & h_\ell(s, 0) & \cdots & h_\ell(s, n_\ell - 2) \\ \vdots & \vdots & \vdots & \ddots & \vdots \\ 0 & 0 & 0 & \cdots & h_\ell(s, 0) \end{pmatrix},$$

where  $h_\ell(s, j)$  is defined as

$$h_\ell(s, j) = \begin{cases} |\lambda_\ell|^s [\cos(\theta_\ell s) + i \sin(\theta_\ell s)] & j = 0 \\ \frac{s!}{j!(s-j)!} |\lambda_\ell|^s [\cos(\theta_\ell s) + i \sin(\theta_\ell s)] & \text{if } s \geq j > 0 \\ 0 & \text{otherwise.} \end{cases}$$

and  $\theta_\ell$  satisfies  $\cos(\theta_\ell) = \operatorname{Re}(\lambda_\ell)/|\lambda_\ell|$  and  $\sin(\theta_\ell) = \operatorname{Im}(\lambda_\ell)/|\lambda_\ell|$  as before.

This representation allows us to write

$$\begin{aligned} F^s = \sum_{j=1}^q \sum_{l=0}^{\min(n_\ell, \lfloor s \rfloor)} & \frac{s(s-1)\cdots(s-l+1)}{l(l-1)\cdots 1} |\lambda_j|^{s-l} \\ & \times \left\{ [B_{jl} \cos(\theta_j s) + C_{jl} \sin(\theta_j s)] + i[D_{jl} \cos(\theta_j s) + E_{jl} \sin(\theta_j s)] \right\} \end{aligned} \quad (10)$$

where the coefficient matrices  $B_{jl}$ ,  $C_{jl}$ ,  $D_{jl}$ , and  $E_{jl}$  are chosen to match  $F^0, F^1, F^2, \dots$ . For integer values of  $s$ , the imaginary components of  $MJ^sM^{-1}$  exactly cancel, so we can use the real part of (10) alone, giving

$$F^s = \sum_{j=1}^q \sum_{l=0}^{\min(n_\ell, \lfloor s \rfloor)} \frac{s(s-1)\cdots(s-l+1)}{l(l-1)\cdots 1} |\lambda_j|^{s-l} [B_{jl} \cos(\theta_j s) + C_{jl} \sin(\theta_j s)] \quad (11)$$

to produce  $F^1, F^2, F^3, \dots$ . Our proposal, in a nutshell, is to use the definition given by (11) for all of the reals rather than just the integers, exactly as we did in the motivating AR(1) examples.

Equation (10) has another practical implication. Although  $F^s$  has real and imaginary components for real  $s$ , we are only interested in its real component that generates the IRFs for integer values of  $s$ . Rather than explicitly calculating the matrices  $B_{jl}$  and  $C_{jl}$  to use (11), we can calculate the complex valued  $F^s$  and simply drop its imaginary component. This calculation is directly available in many programming languages and can be implemented as  $MJ^sM^{-1}$  using the Jordan decomposition if it is not.

We conclude this section with a formal statement of the result.

**Proposition 1** (Impulse Response Functions for VARs). *Let  $F$  be the coefficient matrix of the canonical VAR(1) representation of an arbitrary real-valued VAR( $p$ )  $y_t$ . Define  $\Psi_u(s) = e_{1p} \operatorname{Re}(F^s) e'_{1p} u$  for all  $s \in [0, +\infty)$ , where  $u \in \mathbb{R}^k$  is a shock of theoretical interest. Then  $\Psi_u(s)$  satisfies (1) for all integer values of  $s$  and satisfies the recurrence relation implied by the original VAR for all positive, real values of  $s$ ,*

$$\Psi_u(s) = \sum_{j=1}^q A_j \Psi_u(s-j). \quad (12)$$

*Proof.* The fact that  $\Psi_u(s)$  meets the definition of the IRF on integers is discussed in the text and follows from simple algebra. Observe that the series  $a_s = \operatorname{Re}(F^s) e'_{1p} u$  satisfies  $a_s = Fa_{s-1}$  since  $F$  is real and

$$Fa_{s-1} = F \operatorname{Re}(F^{s-1}) e'_{1p} u = \operatorname{Re}(F^s) e'_{1p} u = a_s.$$

The conclusion of this proposition is a direct consequence.  $\square$

## 2.3 Extensions to other linear models

This section considers three extensions to the previous section. First, we show how to calculate cumulative response functions for VAR( $p$ )s. Second, we show how to calculate

IRFs for Vector Error Correction Models (VECM). And, third, we show how to calculate IRFs for VARMA( $p, q$ ) models. These results all rely on augmenting the series to create a new canonical VAR(1) and can easily be combined and extended further to other recursive linear models.

First, suppose that  $y_t$  has a VAR( $p$ ) representation as before. but we want to derive the effect of the shock  $u$  on  $S_t$ , the cumulative sum of the  $y_t$ s,

$$S_t = \sum_{s=0}^t y_s.$$

Since  $S_t - y_t = S_{t-1}$ , we can extend the canonical representation for  $y_t$  by embedding this relationship as the first element of the vector  $Z_t$  in (8). Equation (8) becomes

$$\begin{pmatrix} S_t - y_t \\ y_t \\ y_{t-1} \\ \vdots \\ y_{t-p+1} \end{pmatrix} = \underbrace{\begin{pmatrix} I & 0 & \cdots & 0 & 0 \\ 0 & A_1 & \cdots & A_{p-1} & A_p \\ 0 & I & \cdots & 0 & 0 \\ \vdots & \vdots & \ddots & \vdots & \vdots \\ 0 & 0 & \cdots & I & 0 \end{pmatrix}}_{F} \begin{pmatrix} S_{t-1} \\ y_{t-1} \\ \vdots \\ y_{t-p+1} \\ y_{t-p} \end{pmatrix} + \begin{pmatrix} 0 \\ \varepsilon_t \\ 0 \\ \vdots \\ 0 \end{pmatrix}$$

and can be rewritten as

$$\begin{pmatrix} S_t \\ y_t \\ y_{t-1} \\ \vdots \\ y_{t-p+1} \end{pmatrix} = \underbrace{\begin{pmatrix} I & A_1 & \cdots & A_{p-1} & A_p \\ 0 & A_1 & \cdots & A_{p-1} & A_p \\ 0 & I & \cdots & 0 & 0 \\ \vdots & \vdots & \ddots & \vdots & \vdots \\ 0 & 0 & \cdots & I & 0 \end{pmatrix}}_F \begin{pmatrix} S_{t-1} \\ y_{t-1} \\ y_{t-2} \\ \vdots \\ y_{t-p} \end{pmatrix} + \begin{pmatrix} \varepsilon_t \\ \varepsilon_t \\ 0 \\ \vdots \\ 0 \end{pmatrix}.$$

This representation is now a VAR(1) that can be handled exactly as in Proposition 1 and  $\Psi_u(s)$  can be defined as  $e_{1,p+1} \text{Re}(F^s)(e_{1,p+1} + e_{2,p+1})' u$

The VECM model has similar behavior. Suppose now that we have the relationship

$$\Delta y_t = B y_{t-1} + A_1 \Delta y_{t-1} + \cdots + A_p \Delta y_{t-p} + \varepsilon_t.$$

This can also be put in a canonical form using almost identical arguments as before,

$$\begin{pmatrix} y_t \\ \Delta y_t \\ \Delta y_{t-1} \\ \vdots \\ \Delta y_{t-p+1} \end{pmatrix} = \underbrace{\begin{pmatrix} (I+B) & A_1 & \cdots & A_{p-1} & A_p \\ B & A_1 & \cdots & A_{p-1} & A_p \\ 0 & I & \cdots & 0 & 0 \\ \vdots & \vdots & \ddots & \vdots & \vdots \\ 0 & 0 & \cdots & I & 0 \end{pmatrix}}_F \begin{pmatrix} y_{t-1} \\ \Delta y_{t-1} \\ \vdots \\ \Delta y_{t-p+1} \\ \Delta y_{t-p} \end{pmatrix} + \begin{pmatrix} \varepsilon_t \\ \varepsilon_t \\ 0 \\ \vdots \\ 0 \end{pmatrix}$$

and  $\Psi_u(s)$  can be defined as  $e_{1,p+1} \operatorname{Re}(F^s)(e_{1,p+1} + e_{2,p+1})' u$  again.

VARMA( $p, q$ )s can also be handled similarly. If  $y_t$  satisfies

$$y_t = \sum_{j=1}^p A_j y_{t-j} + \sum_{i=1}^q B_i \varepsilon_{t-i} + \varepsilon_t$$

this can be written as a canonical VAR(1) using the equation

$$\begin{pmatrix} y_t \\ y_{t-1} \\ \vdots \\ y_{t-p+1} \\ x_t \\ x_{t-1} \\ \vdots \\ x_{t-q+1} \end{pmatrix} = \underbrace{\begin{pmatrix} A_1 & \cdots & A_{p-1} & A_p & B_1 & \cdots & B_{q-1} & B_q \\ I_k & \cdots & 0 & 0 & 0 & \cdots & 0 & 0 \\ \vdots & \ddots & \vdots & \vdots & \vdots & & \vdots & \vdots \\ 0 & \cdots & I_k & 0 & 0 & \cdots & 0 & 0 \\ 0 & \cdots & 0 & 0 & 0 & \cdots & 0 & 0 \\ 0 & \cdots & 0 & 0 & I_k & \cdots & 0 & 0 \\ \vdots & & \vdots & \vdots & \vdots & \ddots & \vdots & 0 \\ 0 & \cdots & 0 & 0 & 0 & \cdots & I_k & 0 \end{pmatrix}}_F \begin{pmatrix} y_{t-1} \\ y_{t-p+1} \\ \vdots \\ y_{t-p} \\ x_{t-1} \\ \vdots \\ x_{t-q+1} \\ x_{t-q} \end{pmatrix} + \begin{pmatrix} \varepsilon_t \\ 0 \\ \vdots \\ 0 \\ \varepsilon_t \\ 0 \\ \vdots \\ 0 \end{pmatrix}.$$

Now  $\Psi_u(s) = e_{1,p+q} \operatorname{Re}(F^s)(e_{1,p+q} + e_{p+1,p+q})' u$ .

Other extensions are obviously also possible and these results can be applied to state space models as well. See Hansen and Sargent (2013) for additional examples and discussion.

### 3 Examples

In this section, we present two examples. The first is a numerical example that demonstrates how these methods scale when they are used to graph many curves simultaneously. The second is an application to Uhlig's (2005) partial identification strategy for monetary policy shocks.

### 3.1 Numerical example

For a simple numerical example, consider the two-variable VAR(2)

$$\begin{pmatrix} y_{1t} \\ y_{2t} \end{pmatrix} = \begin{pmatrix} -0.50 & 0.01 \\ 0.30 & 0.10 \end{pmatrix} \begin{pmatrix} y_{1,t-1} \\ y_{2,t-1} \end{pmatrix} + \begin{pmatrix} -0.20 & 0.10 \\ -0.10 & 0.00 \end{pmatrix} \begin{pmatrix} y_{1,t-2} \\ y_{2,t-2} \end{pmatrix} + \begin{pmatrix} \varepsilon_{1t} \\ \varepsilon_{2t} \end{pmatrix} \quad (13)$$

and assume that  $(\varepsilon_{1t}, \varepsilon_{2t}) \sim N(0, I)$  represents the shocks of interest.

The IRF for an  $\varepsilon_1$ -shock is defined as described above,

$$\Psi_1(s) = e_{1,2} \operatorname{Re}(F^s) e'_{1,2} \begin{pmatrix} 1 \\ 0 \end{pmatrix}$$

with

$$F = \begin{pmatrix} -0.50 & 0.01 & -0.20 & 0.10 \\ 0.30 & 0.10 & -0.10 & 0.00 \\ 1.00 & 0.00 & 0.00 & 0.00 \\ 0.00 & 1.00 & 0.00 & 0.00 \end{pmatrix}$$

Similarly, the IRF for an  $\varepsilon_2$ -shock is given by

$$\Psi_2(s) = e_{1,2} \operatorname{Re}(F^s) e'_{1,2} \begin{pmatrix} 0 \\ 1 \end{pmatrix}.$$

We plot the IRFs in the first two columns Figure 3. The first column plots the standard IRFs, using linear interpolation between integer-valued time periods, and the second plots our proposed smooth plots. Although the general impressions from both graphs are similar, there are important differences. First, peaks and troughs are often underestimated by the standard IRFs and their timing is frequently misidentified. This is especially apparent in the first peak in the second row, which falls exactly on period  $t + 1$  using linear interpolation but approximately  $t + 0.5$  using ours. Second, even the sign of the IRF can be misidentified, as we see with the immediate response of  $y_1$  to a shock in  $\varepsilon_2$ .

However, it would be reasonable for researchers to want to emphasize the value of the IRF at the integer time-periods, since those do not depend on any method of interpolation. The third column of Figure 3 demonstrates one method of doing this: plot the individual points of the IRF defined on the integers over a light version of the curve.

The weaknesses of using linear interpolation become more apparent when we graph multiple perturbations of the IRFs in the same panel, which is a common way of representing uncertainty or set-identified responses. To demonstrate this phenomenon, we generated 150 perturbations of the IRFs by adding independent  $N(0, 0.15)$  noise terms to each element of the VAR coefficients in (13), then calculating and plotting the IRFs as before. (The graphs use alpha blending, a form of partial transparency, to make the individual curves more visible.)

These graphs are shown in Figure 4. The same issues apparent in Figure 3 are present here as well. But there are other problems as well. In the first curve, for example, the discrete IRF shows substantial negative correlation between the period 2 and period 3 estimated response and the period 3 and 4 response to an  $\varepsilon_1$ -shock. But the smoothed graph makes it clear that this is driven by the timing and size of the first peak. When that peak is near period 2, the curve has time to fall noticeably before period 2, but when the peak is closer to period 3, the curve is still rising for that interval. The actual dynamics implied by the different curves are very similar. Similar but less dramatic distortions appear in the other panels as well. In the third row, for example, the discrete IRF shows that about half of the parameter values have an initial increase in response to a  $\gamma_{20}$  shock and half have an initial decrease, but the smooth curves show that virtually all of them have an immediate decrease, but that many start to increase very soon. The exact location of the peak that falls between periods 1 and 2 determines most of the initial dynamics, but this is impossible to see in the discrete curve.

These graphs reveal that our method of constructing IRFs is more resilient to perturbation than linear interpolation: curves generated by close coefficient values have a more similar appearance. This property is particularly useful when graphing many similar curves to represent statistical uncertainty. Moreover, as the right columns in Figures 3 and 4 illustrate, it is still possible to emphasize the integer-valued time periods while using our method of interpolation.

### 3.2 Empirical analysis of the effect of monetary policy

This section demonstrates our proposed method for constructing IRFs in a widely-studied empirical setting. We conduct a brief analysis of the effect of monetary policy on the real economy using Uhlig's (2005) sign-restriction partial identification strategy.

First, a quick review. In Structural VAR models, the shocks of theoretical interest — a monetary policy shock in this section — can simultaneously affect all of the variables in the model. Without additional assumptions beyond those necessary to estimate the

coefficients of the VAR, we can not estimate all of the unknown parameters necessary to identify the shock.<sup>4</sup> I.e., if  $y_t$  is a VAR( $p$ ),

$$y_t = \alpha + \sum_{i=1}^p A_i y_{t-p} + \varepsilon_t, \quad (14)$$

with  $\varepsilon_t \sim (0, \Sigma)$  a martingale difference sequence, then  $\varepsilon_t$  is related to the sequence of theoretical shocks  $\delta_t$  through

$$\varepsilon_t = \Gamma \delta_t$$

and  $\delta_t \sim (0, I)$  is also martingale difference sequence. The variance covariance matrix,  $\Sigma$ , can be consistently estimated, but  $\Gamma$  will in general have more unique elements than  $\Sigma$ . The IRF corresponding to a vector of theoretical shocks  $\delta$  is given by

$$\Psi_\delta(s) = e_{1p}' \text{Re}(F^s) e_{1p} \Gamma \delta \quad (15)$$

so additional restrictions on  $\Gamma$  are necessary to estimate  $\Psi_\delta$ .

Uhlig (2005) proposes using a minimal set of assumptions to identify *potential* monetary policy shocks. Letting the first element of  $\delta$  represent a positive monetary policy shock, Uhlig's approach is to generate candidate shocks randomly and calculate  $\Psi_\delta$  corresponding to that specific shock. IRFs that match some a priori plausible criteria are kept as potential responses to monetary policy shocks and the resulting set of functions partially identifies the effect of a shock. Formally, for given estimates  $\hat{F}$  and  $\hat{\Sigma}$ , this procedure amounts to generating many candidate shocks  $u^* = u / \|u\|_2$  where  $u \sim N(0, I)$  and calculating the candidate IRFs as

$$\hat{\Psi}_{u^*}(s) = e_{1p}' \text{Re}(\hat{F}^s) e_{1p}' \hat{\Sigma}^{1/2} u^*, \quad (16)$$

then discarding  $\hat{\Psi}_{u^*}(s)$  that do not meet a set of criteria of that define and constrain the monetary policy shock.

In this paper, we use our proposed method for graphing IRFs to plot the candidate responses to a monetary policy shock using Uhlig's sign restrictions. We fit a 6-lag VAR using the same six variables as Uhlig: real GDP, the GDP deflator, the federal funds rate, borrowed reserves, nonborrowed reserves, and a commodity price index.<sup>5</sup> We also impose the same restrictions as Uhlig:

---

<sup>4</sup>Kilian (2013) gives a recent review of the SVAR literature.

<sup>5</sup>As in Uhlig, we fit the model in levels and without an explicit time trend.

- the Federal Funds rate does not increase for five months after a monetary policy shock,
- the price level does not decrease for five months after a monetary policy shock, and
- nonborrowed reserves does not decrease after a monetary policy shock.

Since our interest here is in the method of displaying IRFs, we use Bernanke and Mihov's original dataset, which covers January 1965 through December 1997. Most of the variables are available monthly. Since GDP and the GDP deflator are only quarterly, their values are interpolated as described by Bernanke et al. (1997) and Bernanke and Mihov (1998) and we fit a VAR on the monthly data.

Figure 5 presents our graphs.<sup>6</sup> For this exercise, we only present the estimate of the identified set that is associated with the OLS point estimates and ignore the additional uncertainty in estimating the coefficients. The main results are essentially already known: the immediate effect of a sign-identified monetary policy shock on GDP is ambiguous in the very short run but lowers GDP relative to trend after about two years. And the effects on the other variables are consistent with the identification strategy and with the previous literature. But our approach to smoothing the IRFs allows each of the individual candidate shocks to be studied as well. Many of the curves have a minimum between 1/2 to 2 years, but there is considerable uncertainty over the exact date of the minimum. The dynamics expressed by the outer envelope of the curves, which is the quantity plotted in many VAR applications, is not particularly representative of any of the individual IRFs.

## 4 Conclusion

Vector Autoregressive models do not just have implications for the period-to-period dynamics of a stochastic process, they also have implications about the very short-run dynamics within periods. In this paper, we propose that researchers graph those intra-period dynamics when plotting the IRFs for linear models and we give a simple method to do so, based on the model's canonical VAR(1) representation. Even when researchers do not want to assign any economic importance to these ultra short-run dynamics, plotting them in the IRFs minimizes visual distortions that can arise from discretizing the dynamics, especially when several IRFs are plotted over each other to represent uncertainty or partial identification.

---

<sup>6</sup>As in our earlier example, these graphs use partial transparency, alpha blending, to show as many of the individual curves as possible.

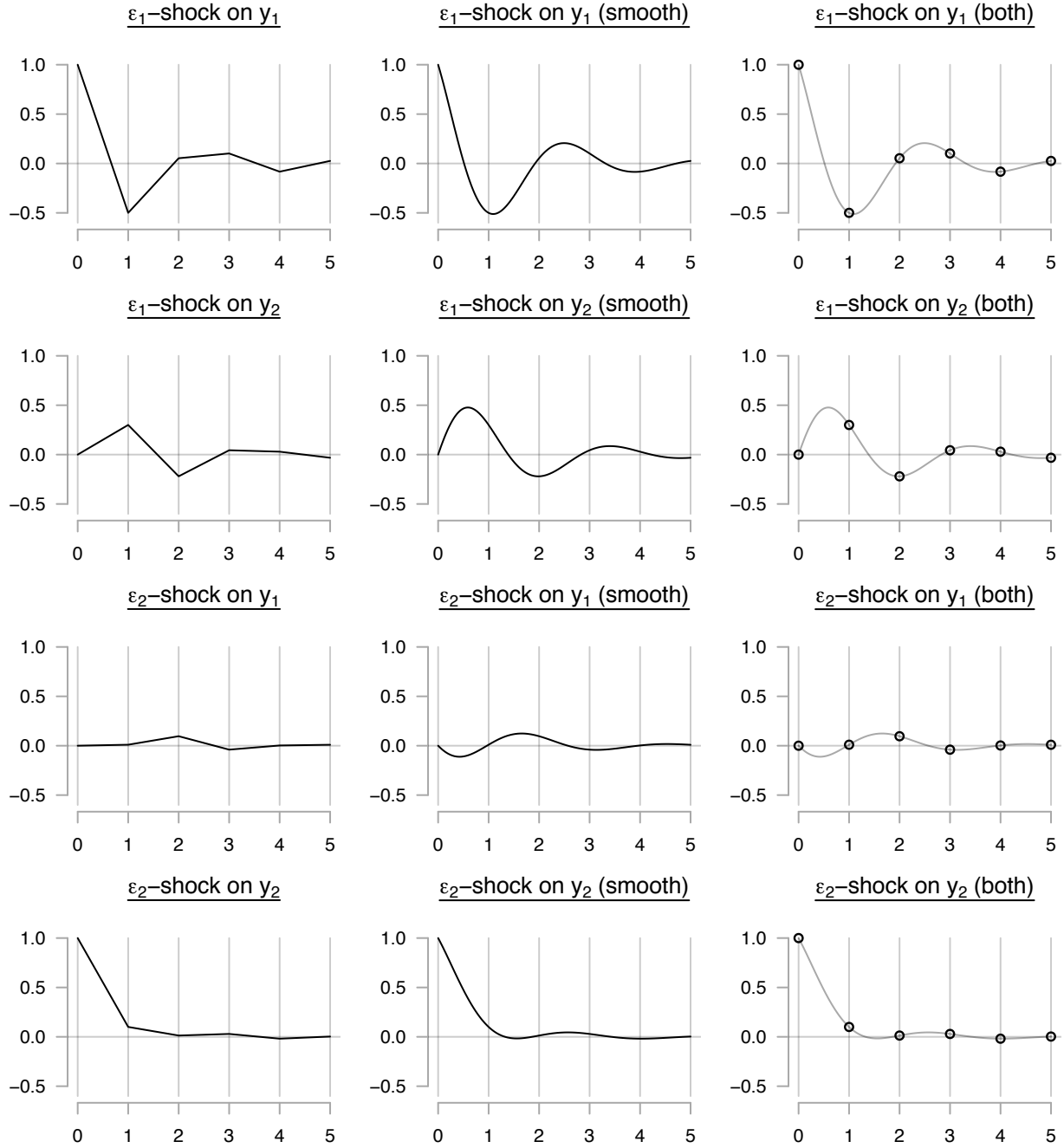


Figure 3: Impulse Response Functions from Section 3.1 example;  $y_t$  is generated by Equation (13). The left column plots standard IRFs, the middle column plots our new method, and the right column plots our new approach, emphasizing the values at integer time periods.

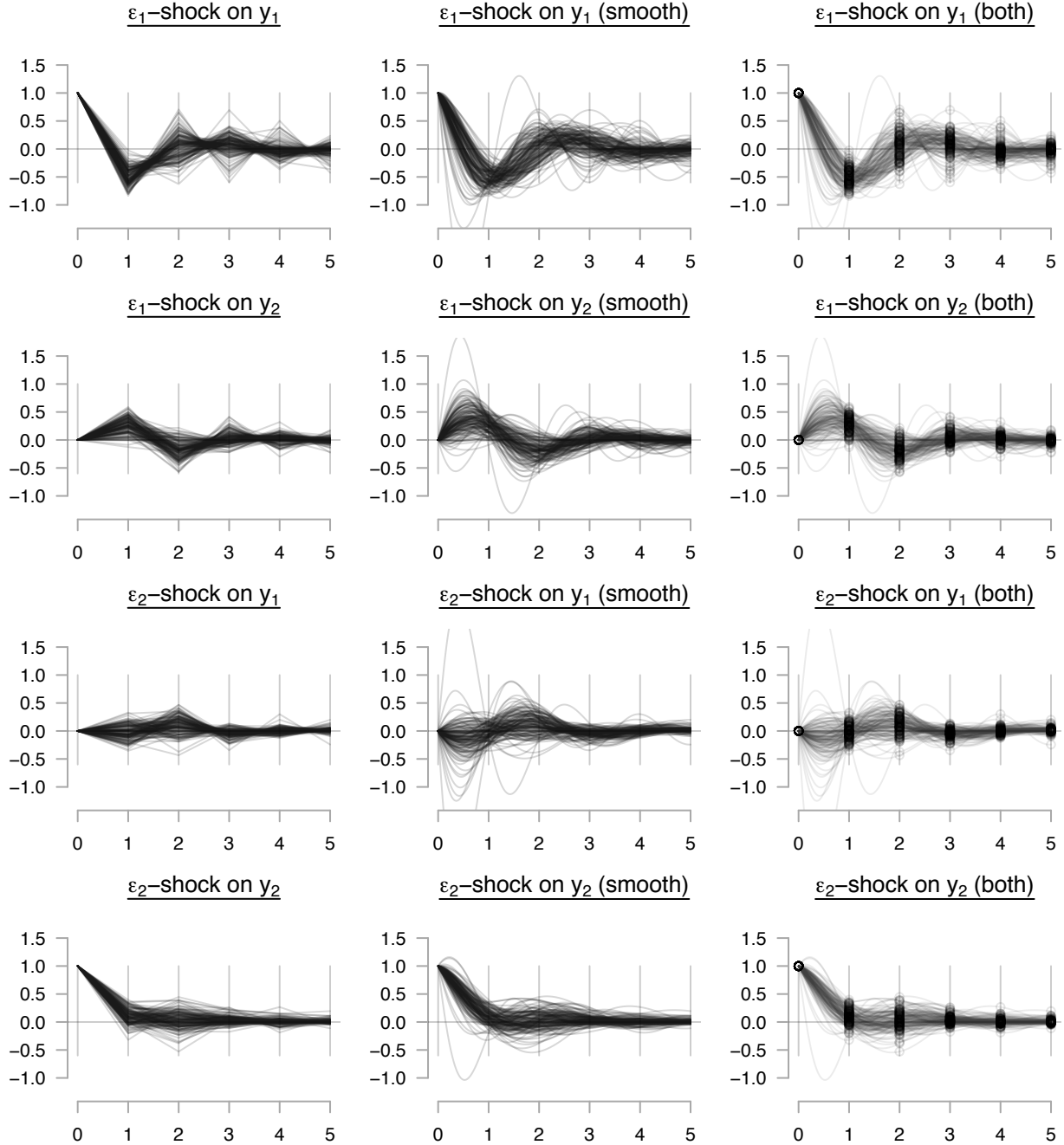


Figure 4: Impulse Response Functions from Section 3.1 example;  $y_t$  is generated by Equation (13) with independent  $N(0, 0.15)$  random variable added to each coefficient. These graphs plot the IRFs from 150 independent draws of the coefficient matrices. The left column plots standard IRFs, the middle column plots our new method, and the right column plots our new approach with an emphasis on the integer time periods..

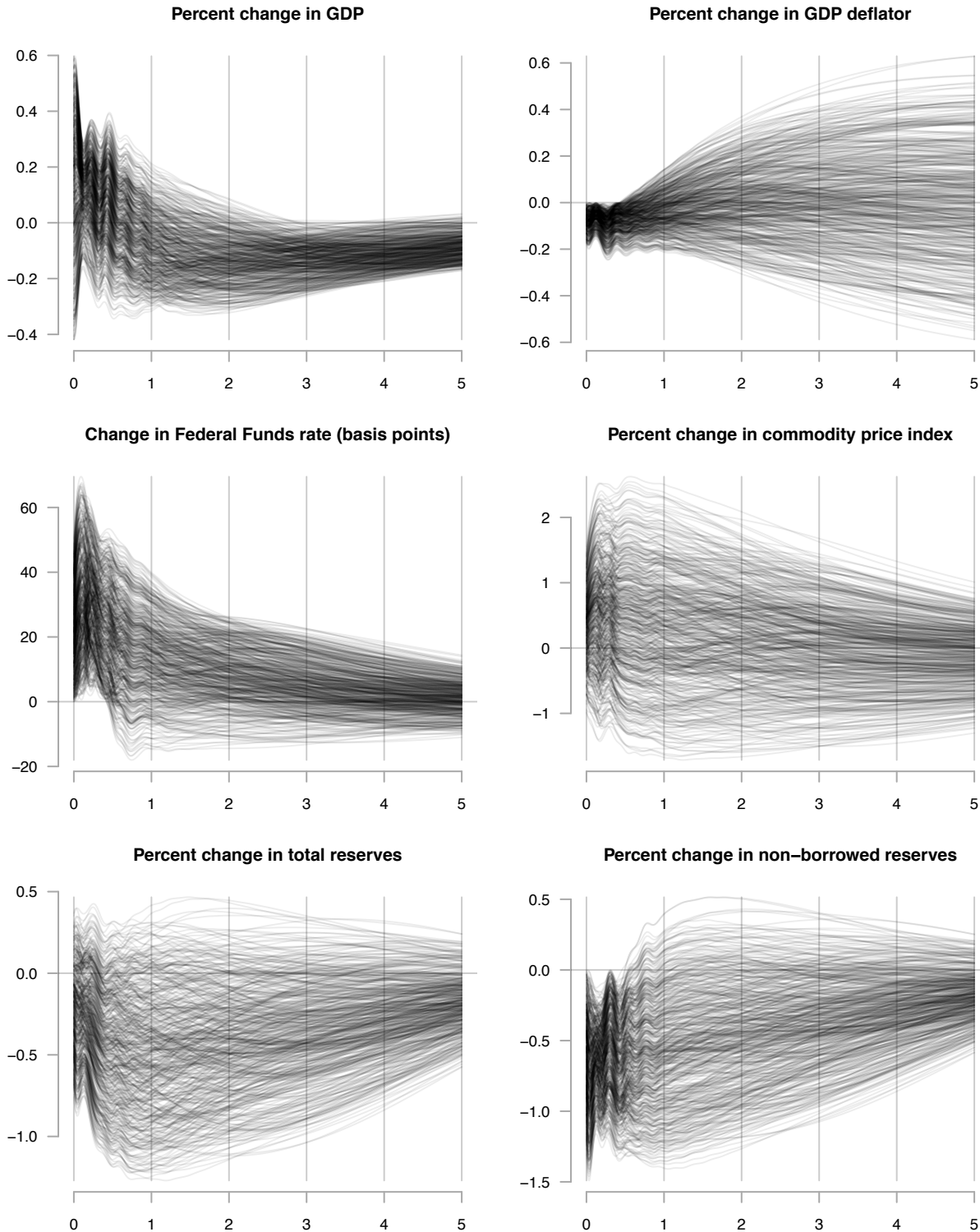


Figure 5: Empirical response of each variable to a sign-identified negative monetary policy shock; see description in Section 3.2. The horizontal axis is the number of years since the initial shock. These figures graph 500 candidate shocks.

## References

- B. S. Bernanke and I. Mihov. Measuring monetary policy. *The Quarterly Journal of Economics*, 113(3):869–902, 1998.
- B. S. Bernanke, M. Gertler, and M. Watson. Systematic monetary policy and the effects of oil price shocks. *Brookings papers on economic activity*, 1997(1):91–157, 1997.
- J. D. Hamilton. *Time Series Analysis*. Princeton University Press, 1994.
- L. P. Hansen and T. J. Sargent. *Recursive models of dynamic linear economies*. Princeton University Press, 2013.
- A. Inoue and L. Kilian. Inference on impulse response functions in structural VAR models. *Journal of Econometrics*, 177(1):1–13, 2013.
- L. Kilian. Small-sample confidence intervals for impulse response functions. *The Review of Economics and Statistics*, 80(2):218–230, 1998.
- L. Kilian. Structural vector autoregressions. In N. Hashimzade and M. A. Thornton, editors, *Handbook of Research Methods and Applications in Empirical Macroeconomics*. Edward Elgar Publishing, Inc., 2013.
- R Development Core Team. *R: A Language and Environment for Statistical Computing*. R Foundation for Statistical Computing, <http://www.R-project.org/>, Vienna, Austria, 2011.
- C. A. Sims and T. Zha. Error bands for impulse responses. *Econometrica*, 67(5):1113–1155, 1999.
- J. H. Stock and M. W. Watson. Vector autoregressions. *Journal of Economic Perspectives*, 15(4):101–115, Fall 2001.
- H. Uhlig. What are the effects of monetary policy on output? Results from an agnostic identification procedure. *Journal of Monetary Economics*, 52(2):381–419, March 2005.

## **A Appendix: Changes to this paper from previous versions**

Latest:

- Rerender pictures to fix display problems in some pdf vieweres.

v0.3, 2016-03-28:

- Makes small wording changes to the abstract.
- Changes the title of the paper.
- Adds empirical analysis of monetary policy (as in Uhlig, 2005).
- Adds Git commit information to the pdf.
- Adds this changelog to the pdf.
- Adds a table of contents to the pdf.
- Makes several small formatting changes.
- Makes several small changes to the internal file organization.

v0.2.2, 2015-02-22: Tweaks the abstract.

v0.2.1, 2015-02-21: Adds author affiliation.

v0.2.0, 2015-02-21: Adds cumulative response function and VECM section; and revises the text of the paper.

v0.1.0, 2015-02-11: First draft of the paper.